

Evolved Galaxies at $z > 1.5$ from the Gemini Deep Deep Survey: The Formation Epoch of Massive Stellar Systems

Patrick J. McCarthy¹, Damien Le Borgne², David Crampton³, Hsiao-Wen Chen^{5,10},
Roberto G. Abraham², Karl Glazebrook⁴, Sandra Savaglio^{4,9}, Raymond G. Carlberg²,
Ronald O. Marzke⁸, Kathy Roth⁶, Inger Jørgensen⁶, Isobel Hook⁷,
Richard Murowinski³ & Stephanie Juneau³

ABSTRACT

We present spectroscopic evidence from the Gemini Deep Deep Survey (GDDS) for a significant population of color-selected red galaxies at $1.3 < z < 2.2$ whose integrated light is dominated by evolved stars. Unlike radio-selected objects, the $z > 1.5$ old galaxies have a sky density $> 0.1 \text{ arcmin}^{-2}$. Conservative age estimates for 20 galaxies with $z > 1.3$; $\langle z \rangle = 1.49$, give a median age of 1.2 Gyr and $\langle z_f \rangle = 2.4$. One quarter of the galaxies have inferred $z_f > 4$. Models restricted to $[\text{Fe}/\text{H}] \leq 0$ give median ages and z_f of 2.3 Gyr and 3.3, respectively. These galaxies are among the most massive and contribute $\sim 50\%$ of the stellar mass density at $1 < z < 2$. The derived ages and most probable

¹Carnegie Observatories, 813 Santa Barbara St, Pasadena, CA 91101, pmc2@ociw.edu

²Department of Astronomy & Astrophysics, University of Toronto, Toronto ON, M5S 3H8 Canada, leborgne@astro.utoronto.ca, abraham@astro.utoronto.ca, carlberg@astro.utoronto.ca

³NRC Herzberg Institute for Astrophysics, 5071 W. Saanich Rd., Victoria, BC, Canada, david.crampton@nrc-cnrc.gc.ca, murowinski@nrc-cnrc.gc.ca, stephanie.juneau@nrc-cnrc.gc.ca

⁴Department of Physics & Astronomy, Johns Hopkins University, Baltimore, MD 21218, kgb@pha.jhu.edu, savaglio@pha.jhu.edu

⁵Center for Space Sciences, Massachusetts Institute of Technology, 70 Vassar St., Bld. 37, Cambridge, MA 02139, hchen@space.mit.edu

⁶Gemini Northern Operations Center, 670 N. A'ohoku Place, Hilo, HI 97620, jorgensen@gemini.edu, kroth@gemini.edu

⁷UK Gemini Operations Center, Keble Road, Oxford University, Oxford, OX 3RH, UK,

⁸Department of Astronomy and Physics, San Francisco State University, San Francisco, CA, 94132, marzke@stars.sfsu.edu

⁹On leave of absence from INAF Osservatorio Astronomico di Roma, Italy

¹⁰Hubble Fellow

star formation histories suggest a high star-formation-rate ($\sim 300 - 500 M_{\odot}\text{yr}^{-1}$) phase in the progenitor population. We argue that most of the red galaxies are not descendants of the typical $z \sim 3$ Lyman break galaxies. Galaxies associated with luminous sub-mm sources have the requisite star formation rates to be the progenitor population. Our results point toward early and rapid formation for a significant fraction of present day massive galaxies.

Subject headings: Galaxies: Formation - Galaxies: Evolution - Galaxies: Abundances - Infrared: Galaxies

1. Introduction

Recent surveys have placed significant constraints on galaxy formation models. The evolving stellar mass density (e.g. Glazebrook et al. 2004, hereafter Paper III; Dickinson et al. 2003; Rudnick et al. 2004; Fontana et al. 2004) now seems in reasonable accord with measurements of integrated star formation rates (e.g. Steidel et al. 1999). Interpretation of these volume-averaged quantities remains difficult, in part because the earliest phases of galaxy formation are poorly understood. Age determinations for galaxies at intermediate and high redshift provide an accurate clock for galaxy formation at early times. Application of this technique has been hampered by the small samples of suitable galaxies at appropriate redshifts, and the difficulty of obtaining reliable age estimates from low signal-to-noise spectra. Age determinations for the prototypical evolved red galaxy, 53W091, range from > 3.5 Gyr (Dunlop et al. 1999; Nolan et al. 2001) to as young as $1 - 1.5$ Gyr (Bruzual & Magris 1997; Yi et al. 2000). Visible-light surveys of galaxies at $z > 1$ are biased against inclusion of red galaxies and hence are limited in their ability to shed light on the formation of the oldest and most massive galaxies. Near-IR surveys of galaxies with red optical-to-IR colors provide the requisite samples of massive galaxies at redshifts that constrain the formation epoch.

Most spectroscopic studies of the red $R - K$ or $I - K$ population to date (e.g. Cimatti et al. 2002; Yan et al. 2004), have not revealed signatures of evolved populations at $z > 1.3$ due to observational limitations. At higher redshifts the strong signatures of older stellar populations (e.g., 4000 \AA break and CaII H&K lines) are beyond the reach of most CCD-based spectrographs. At $z > 2$, strong UV resonance lines are redshifted into the atmospheric passband, allowing identification of UV-bright galaxies. In the intermediate regime, $1.3 < z < 2$, evolved galaxies must be probed with weak photospheric features of MgII, MgI and FeII.

The red galaxy population ¹ (e.g. $I - K > 4$) is a mix of evolved and reddened star forming systems. Estimates of the fraction of star forming galaxies in this population range from 20 - 60% (e.g. Cimatti et al. 2002; Smail et al. 2002; Yan et al. 2004). Although the $z > 2$ red $J - K$ selected galaxy population (e.g. Franx et al. 2003) likely contains evolved objects, those with confirmed redshifts all have strong star formation signatures in their rest-UV spectra (van Dokkum et al. 2003), possibly due to observational limitations. Similarly, the massive K-bright galaxies at $z \sim 2$ from the GOODS and K20 surveys (Daddi et al. 2004) have high inferred star formation rates. The Gemini Deep Deep Survey (GDDS: Abraham et al. 2004, hereafter Paper I), was the first to identify evolved galaxies at $z > 1.5$ in significant numbers (also see Cimatti et al. 2004).

The GDDS is a spectroscopic study of galaxies in the $1 < z < 2$ range within four separate areas of the Las Campanas IR Survey (McCarthy et al. 2001). Very long exposures, using the ‘Nod & Shuffle’ sky cancellation technique yielded high quality spectra from which redshifts could be derived for 272 galaxies with $I < 24.5$ (Vega). Catalogs, field locations, mask design, and sample selection are given in Paper I. Twenty GDDS galaxies with $z > 1.3$ display clear signatures of old stellar populations. In this paper we present spectra of these galaxies along with preliminary age determinations and consider the implications of these results for our understanding of the formation of massive galaxies.

2. Quiescent Red Galaxies at $z > 1.3$

The sample of 20 GDDS galaxies with $z > 1.3$ with spectra characteristic of old populations is listed in Table 1. The object designation is given in the first column, followed by the redshift. Confidence classes and spectral classifications are given in Paper I. High confidence redshifts were determined for 71% (75/105) of the $I - K > 3.5$ galaxies and 67% (35/52) of the $I - K > 4$ subsample. These two samples span the redshift range from 0.8-2.1. Among objects with spectroscopic redshifts, 51% of the $I - K > 3.5$ sample have unambiguous old stellar components. The redder galaxies ($I - K > 4$) show an even greater preponderance for pure-old spectra with 72% having significant old populations. About half of the objects with $I - K > 3.5$ and $z > 1.3$ have old spectra, while 80% of the objects with $I - K > 4$ and $z > 1.3$ have old spectral classifications. *Thus 50-80% of the $z > 1.3$ red GDDS sample show spectra with contributions from old stellar populations.* The contribution of old stars in our $z > 1.3$ sample is similar to that seen in the $z \sim 1 - 1.3$ samples (e.g., Cimatti et al. 2002; Yan et al. 2004).

¹A review of the red near-IR selected population can be found in McCarthy (2004).

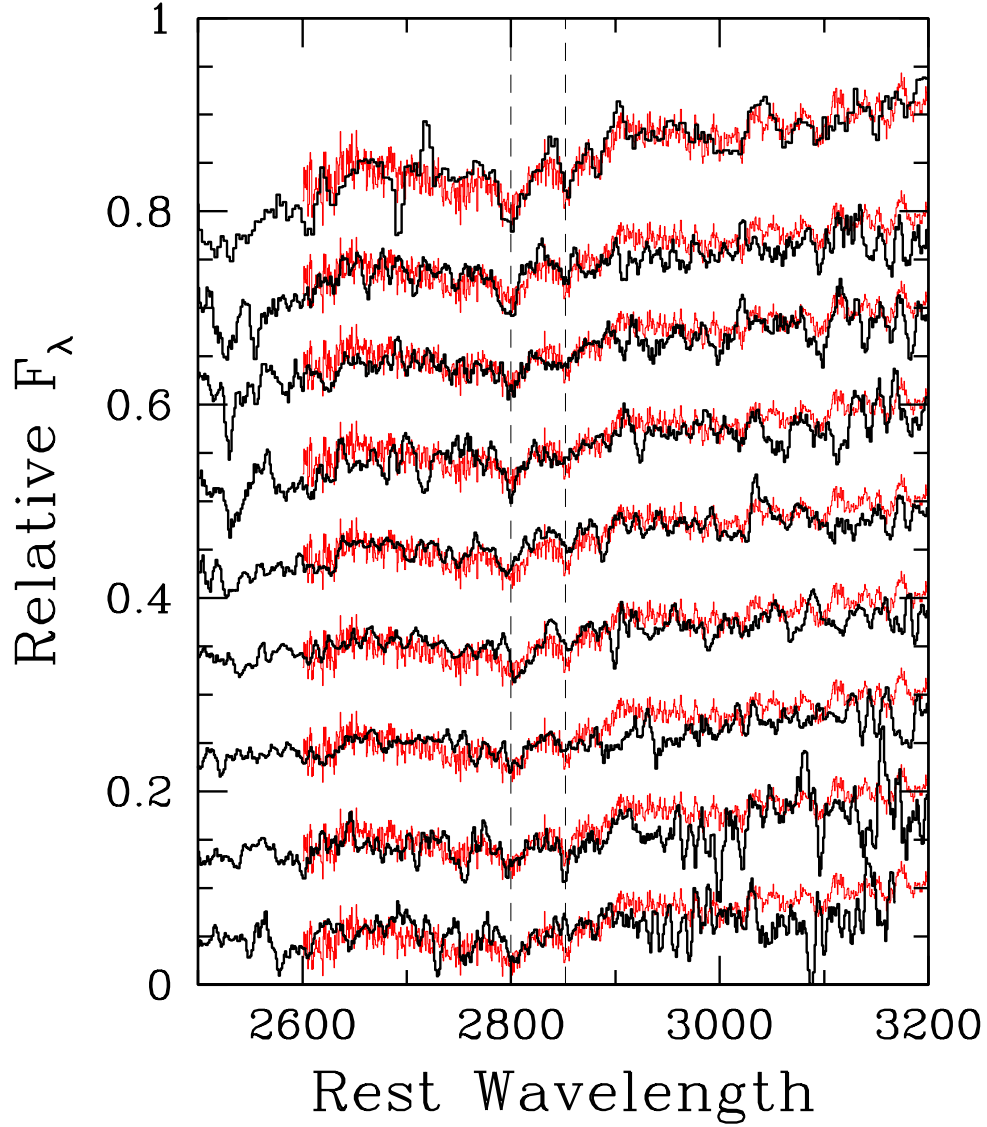


Fig. 1.— Spectra of evolved GDDS galaxies with $z > 1.3$. From top to bottom the objects shown are: GDDS-02-1255, 22-0189, 22-0674, 12-5869, 12-6072, 12-8895, 15-4367, 15-7543, 15-5005. This includes all of the galaxies in Table 1 with $1.49 < z < 2.0$, plus GDDS-02-1255 ($z = 1.34$). The SDSS LRG composite has been overlaid on each spectrum and an offset has been applied to each, in steps of $10^{-18} \text{ erg s}^{-1} \text{ cm}^{-2} \text{ \AA}^{-1}$. The locations of the stellar MgII2800 and MgI2852 lines are indicated by the dashed lines.

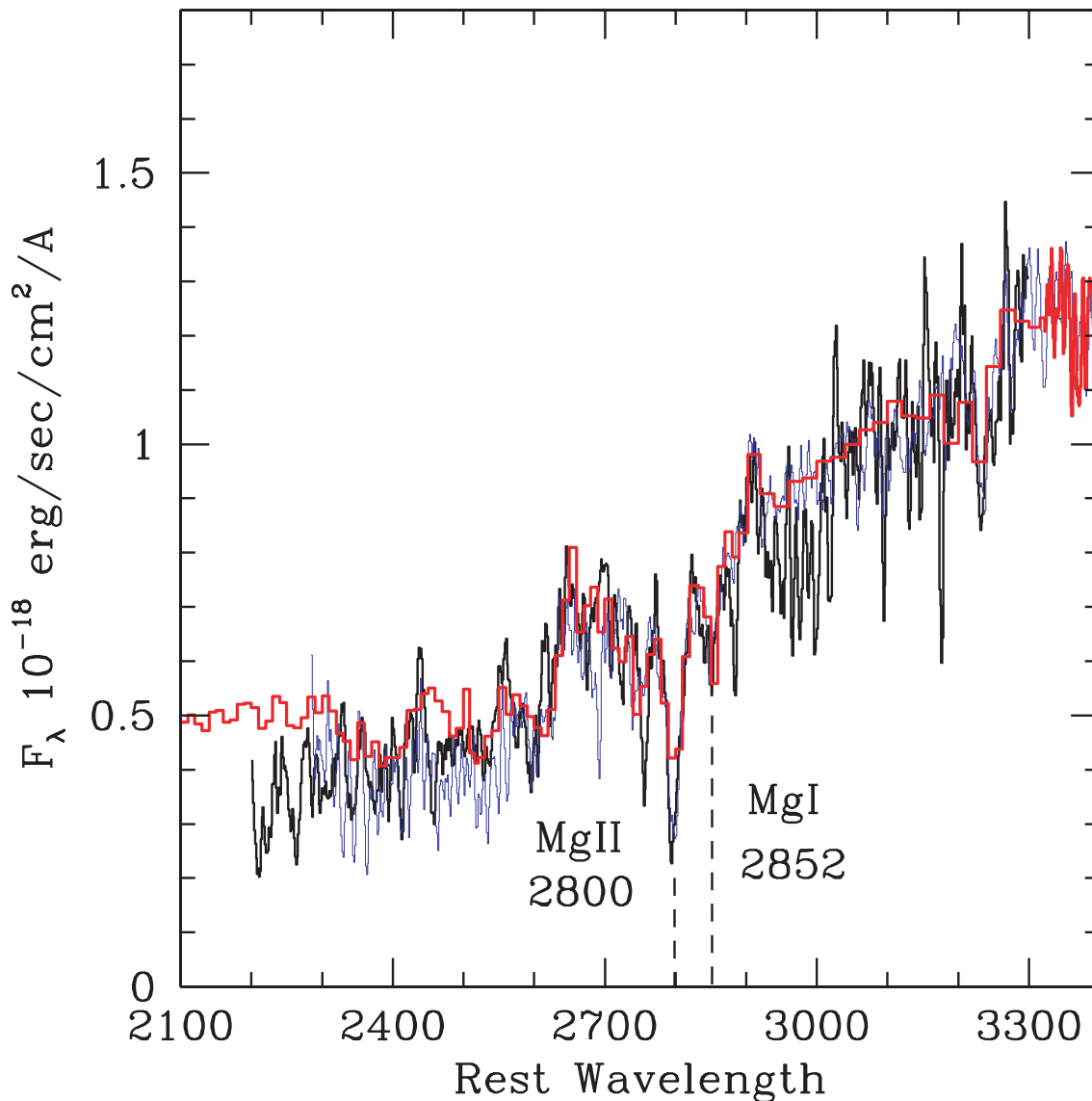


Fig. 2.— Composite spectra of evolved galaxies with $1.3 < z < 1.4$ (in blue, from galaxies GDDS-12-6131, 02-1255, 12-5836, 15-7972, 22-2587, and 12-8025), and $1.6 < z < 1.9$ (in black, from the five objects listed in Table 1 in this redshift range). Both composite spectra show strong MgII2800, MgI2852 absorption and broad spectral features due primarily to FeII absorption. Overlaid in red is a single-burst Bruzual & Charlot (2003) spectral synthesis model with an age of 2 Gyr, solar abundances, and a Salpeter (1955) IMF cutoff at $120M_{\odot}$.

2.1. Individual and Composite Spectra

In Figure 1 we show spectra of 9 $z > 1.3$ objects with high-confidence redshifts and spectral classes indicative of old populations from the four GDDS fields. Over-plotted on these spectra is the SDSS/LRG template (Eisenstein et al. 2003). The evolved GDDS galaxies form a fairly homogeneous set and are reasonably well matched to the SDSS/LRG template. The strongest features in the spectra are the MgII2800 doublet and MgI2852. Numerous weak FeII features blend together to produce a modulated shape to the continuum. The overall spectral slopes and shapes of the objects with $z = 1.6 - 1.8$ are not very different from those at $z = 1.3$, although they have somewhat flatter spectral slopes at $\lambda < 2800\text{\AA}$.

In Figure 2 we show composite spectra of six galaxies from Table 1 with $1.3 < z < 1.4$, and another composite of the five at $1.6 < z < 1.9$. The equivalent widths of the MgII and MgI lines and overall continuum shapes are quite similar. A spectral synthesis model derived using Bruzual & Charlot (2003) is shown over-plotted in red in Figure 2. This reddening-free single-burst simple stellar population model, with an age of 2 Gyr, a Salpeter (1955) IMF and solar abundances, is the youngest solar-abundance model that fits the data well. Older models (e.g. ages of 3 – 4 Gyr) fit the far-UV end of the spectrum better than the 2 Gyr model does, but not at a level that allows us to rule out the 2 Gyr model. Younger models (e.g., 1 Gyr) are bluer than the observed composite spectra. The characteristic ages derived from the composite spectra are consistent with the results from fits to the spectra and broad-band energy distributions of individual objects (Sec. 3.1).

Figures 1 and 2 convey the key result presented in this paper: there is a significant population of color-selected luminous field galaxies at $1.3 < z < 2$ with spectra dominated by old stars. Unlike radio-selected evolved galaxies at $z \sim 1.5$ previously reported (e.g. Dunlop et al. 1996), our objects have a high surface density on the sky (> 0.1 sq. arcmin⁻²).

3. Model Ages and Formation Redshifts

The existence of massive galaxies at redshifts up to $z \sim 2$ with evolved spectra argues for an early formation episode and strains semi-analytic CDM models (e.g. Cole et al. 2000; Baugh et al. 2003). The most successful models (Somerville et al. 2004) can produce sufficiently massive galaxies at early epochs, but still have difficulties in producing red and old galaxies at $z > 1$. The critical empirical issue is understanding the age of the stellar populations, and hence the formation redshifts, in the old red galaxies at the highest redshifts possible.

We made a preliminary attempt to derive very conservative (i.e. minimum) ages for

the galaxies listed in Table 1 by making use of both the information in the spectra and $B - K_s$ photometry. For each galaxy, we systematically compared the observed SED with a set of synthetic spectra computed with PÉGASE.2 (Fioc & Rocca-Volmerange 1997) and constructed a multi-dimensional χ^2 surface spanning a wide range of star-formation histories, ages, extinction (A_v) and metallicities.

The observed SED of each galaxy comprises a flux-calibrated GDDS spectrum and a broad-band spectral energy distribution combined with weights assigned in proportion to the band-width of the observations. In most cases the spectra and broad-band photometry carry nearly equal weight. All the models use a Salpeter (1955) IMF with an upper-mass cutoff of $120M_\odot$. The effects of reddening were modeled by using the Calzetti (1997) extinction law with $A_v = 0 - 1\text{mag}$. Instantaneous-burst models with 12 metallicities ranging from 20% to 175% of solar were considered, together with exponentially declining star formation histories with 10 e-folding times ranging between 0.1 Gyr and 3 Gyr.

From the χ^2 surface, a best-fit age, star formation history, metallicity and extinction were derived. The range of acceptable ages for a given galaxy was limited by the age of the universe at its observed redshift. Statistical uncertainties on the age were computed from the set of models satisfying $\Delta\chi^2 < 3\sigma$. An extensive description of the underlying models and our approach to fitting data to these will be given in Le Borgne et al. (in preparation).

3.1. Results

We summarize the results of our age determination analysis using the PÉGASE.2 models in Table 1. In column 6 of Table 1 we list the best-fit ages and the range of acceptable ages. Bruzual & Charlot (2003) instantaneous-burst models yield best fits with age differences smaller than 0.2 Gyr. Columns 7 through 11 give the e-folding time, A_v , abundance, χ^2 value and formation redshift for the best-fitting models, respectively. The reduced χ^2 values exceed unity, in part, because of imperfections in the model spectral libraries. The formation redshifts are determined from the redshift of observation, the best-fit age and the age of the Universe in a $\Omega_\Lambda = 0.7, \Omega = 0.3, H_0 = 70 \text{ km s}^{-1}\text{Mpc}^{-1}$ cosmology. In nearly all cases the best fits were achieved with either an instantaneous burst or a short e-folding time exponential burst ($< 0.5 \text{ Gyr}$), with a preponderance favoring the instantaneous-burst models.

The single-burst and exponential model fits generally favor metallicities higher than 50% solar. Super solar metallicities reduced the χ^2 values in $\sim 30\%$ of the cases. We truncated our metallicity search space at $[\text{Fe}/\text{H}] = 0.25$. While large values are seen in the

cores of local ellipticals (e.g. Thomas et al. 2003), the large apertures of our spectroscopic and photometric measurements (10 – 20kpc diameter) and the abundance gradients seen in ellipticals produce luminosity weighted abundances within our apertures that are closer to solar (see Jørgensen et al. 1997; Arimoto et al. 1997). For the four objects that favor models with $[\text{Fe}/\text{H}] > 0.15$, fits with the metallicity capped at the solar value yield best-fit ages that are 0.5-1.0 Gyr older than those listed in Table 1.

We have measured the mass-density in high-mass objects and determined the contribution from the $I - K > 3.5$ objects using the procedures from Paper III. Adopting a threshold of $5 \times 10^{10} M_{\odot}$ (for which our sample is mass-complete over the interval $1.3 < z < 2$) we find that the red objects in this sample contribute 49% of the overall stellar mass density.

The median derived age and formation redshifts are 1.2 Gyr and 2.4, respectively for our conservative analysis. Nearly 1/3 of the objects (5/20) have inferred $z_f > 4$. Imposing a minimum collapse time of 3×10^8 yr moves the median formation redshift from 2.4 to ~ 3.0 . Limiting the models to $[\text{Fe}/\text{H}] \leq 0$ shifts the inferred median age and z_f to 2.3 Gyr and 3.2, respectively; imposing $A_v = 0$ in addition yields a median z_f of 4.0.

4. Discussion

The spectra of the red GDDS galaxies reveal unambiguous evidence for old and metal-rich galaxies over the full range from $1 < z < 2$. Our preliminary, conservative analysis implies early and rapid formation for a substantial fraction of these. The median z , age, z_f , and mass for the sample in Table 1 are 1.49, 1.5 Gyr, 2.5, and $1 \times 10^{11} M_{\odot}$, respectively. Our models strongly favor instantaneous bursts in roughly 50% of the objects and short e-folding times (e.g. 0.5 Gyr) for the remaining galaxies. More plausible models, those with star formation extended over one or more dynamical times, produce best-fitting ages that are typically 1 Gyr *larger* than those in Table 1, implying $\langle z_f \rangle \sim 4$ for a substantial fraction of the galaxies.

Taking the z_f in Table 1 as indicative of the onset of star formation, the “median” red galaxy requires a constant star formation rate of $50 M_{\odot} \text{ yr}^{-1}$ over the full 1.5 Gyr period from $z = 2.4$ to $z = 1.5$ to produce the required stellar mass. These rates are higher than that of a typical Lyman Break Galaxy (LBG) at $z \sim 3$ (e.g. Shapley et al. 2003). Constant star formation rate models, however, reproduce neither the colors nor the spectra of the red galaxies. Star formation with an e-folding time of 3×10^8 yr implies peak SFRs $\sim 300 - 500 M_{\odot} \text{ yr}^{-1}$ at $z \sim 2 - 4$ in the most massive galaxies. These high star formation rates, coupled with the strong clustering of the red galaxy population (e.g. McCarthy et al.

2001) and the differences in stellar mass, suggest that these objects are probably not closely connected with the $z = 3 - 4$ Lyman-break galaxy population.

Assembly of the massive GDDS galaxies from many sub-units still requires early, and short-lived, star formation, although the units could be smaller than the typical $8 \times 10^{10} M_{\odot}$ of the GDDS galaxies. While star formation in smaller sub-galactic units will proceed with shorter dynamical times, the best-fitting instantaneous burst (or even $\tau = 0.1$ Gyr) models imply impressive synchronization in the truncation of star formation among the precursors. The near-solar metallicities required to fit the strong UV stellar lines and the favored single-burst models naively argue for a single massive star formation episode (per galaxy) at $2 < z < 5$ as the simplest formation scenario.

It appears that there is a continuous coeval population of massive red galaxies that are traced, in order of decreasing redshift, by: $z > 2$ red $J - K$ galaxies, red GDDS galaxies at $z \sim 1.3 - 2$ and the classical “EROs” at $0.9 < z < 1.3$ observed in the K20, LCIR and other surveys. These all point to an early formation epoch for the progenitors of present day massive galaxies. Our analysis implies high peak star formation rates at $z \geq 2$. At present the only candidates for such rapidly forming massive galaxies at high redshift are the sub-mm luminous sources. The median redshift ($\langle z \rangle = 2.4$) for the bright SCUBA sources (Chapman et al. 2003) is indistinguishable from our current conservative $\langle z_f \rangle$ estimate for the red GDDS galaxies. A significant fraction of the GDDS galaxies, however, appear to have formation redshifts outside the range of known SCUBA redshifts. The $n(z)$ of the SCUBA sources, however, has an inferred tail to $z > 4$ and these may evolve into the red $z > 1.5$ population. In summary, the GDDS has revealed a population of evolved galaxies at $z > 1.5$ and conservative age estimates yield a modest $\langle z_f \rangle$ and point to formation of massive galaxies in episodes of intense star formation.

5. Acknowledgments

This paper is based on observations obtained at the Gemini Observatory, which is operated by AURA Inc., under a cooperative agreement with the NSF on behalf of the Gemini partnership: the NSF (US), PPARC (UK), NRC (Canada), CONICYT (Chile), ARC (Australia), CNPq (Brazil) and CONICET (Argentina). This paper is also based on observations obtained at the Las Campanas Observatory of the Carnegie Institution of Washington. KG and SS acknowledge support from the David and Lucille Packard Foundation, RGA acknowledges support from the NSERC.

REFERENCES

- Abraham, R. G., et al. 2004, *AJ*, 127, 2455 (Paper I)
- Arimoto, N., Matsushita, K., Ishimaru, Y., Ohashi, T., & Renzini, A. 1997, *ApJ*, 477,
- Baugh, C. M., Benson, A. J., Cole, S., Frenk, C. S., & Lacey, C. 2003, *The Mass of Galaxies at Low and High Redshift*, 91
- Bruzual, G., Charlot, S., 2003, *MNRAS*, 344, 1000
- Bruzual, G. & Magris, GC 1997, in “The Ultraviolet Universe at Low and High Redshift : Probing the Progress of Galaxy Evolution” AIP conf. proceedings, 408, 291
- Calzetti, D. 1997, *AJ*, 113, 162.
- Chapman, S., C., Blain, A. W., Ivison, R. J., & Smail. I. R. 2003, *NATURE*, 422, 695
- Cimatti, A., et al. 2004, *Nature*, 430, 184
- Cimatti, A., et al. 2002, *A&A* 381, L68.
- Cole, S., Lacey, C. G., Baugh, C. M., & Frenk, C. S. 2000, *MNRAS*, 319, 168
- Daddi, E., et al. 2004, *ApJ*, 600, 127
- Dickinson, M., Papovich, C., Ferguson, H. C., Budavari, T. 2003, *ApJ*, 587, 25
- Dunlop, J., Peacock, J., Spinrad, H., Dey, A., Jimenez, R., Stern, D., Windhorst, R. 1996, *Nature*, 381, 581
- Eisenstein, D. J., et al. 2003, *ApJ*, 585, 694.
- Fontana, A., et al. 2004, *A&A*, in press (astro-ph/0405055).
- Fioc, M. & Rocca-Volmerange, B. 1997, *A&A* 326, 95
- Franx, M., et al. 2003, *ApJ*, 587, L79
- Glazebrook, K., et al. 2004, *Nature*, 430, 181 (Paper III)
- Jørgensen, I. 1997, *MNRAS*, 288, 161
- McCarthy, P. J. 2004, *ARAA*, Vol. 42, 477.
- McCarthy, P. J., et al. 2001, *ApJ*, 560, L131.

- Nolan, LA; Dunlop, J.S.; Jimenez, R 2001, MNRAS, 323, 385
- Rudnick, G., et al. 2003, ApJ, 599, 847.
- Salpeter, E. E. 1955, ApJ, 121, 161
- Shapley, A., Steidel, C., Pettini, M., Adelberger, K. L., 2003, ApJ, 588, 65
- Smail, I; Owen, F N Morrison, G E; Keel, W C; Ivison, RJ; Ledlow, MJ 2002, ApJ, 581, 844
- Somerville, R. S. et al. 2004, ApJ, 600, 135
- Steidel, C. C., Adelberger, K., Giavalisco, M., Dickinson, M., Pettini, M. 1999, ApJ, 519, 1
- van Dokkum, P G, et al. 2003, ApJ, 587, L83
- Yan, L., & Thompson, D. 2003, ApJ, 586, 765
- Yan, L., Thompson, D., & Soifer, B. T. 2004, AJ in press
- Yi, S, Brown, TM, Heap, S., Hubeny, I, Landsman, W, Lanz, T, Sweigart, A 2000, ApJ, 533, 670

Table 1: Best Fitting Ages for Red Galaxies.

Object	z	K	I-K	Mass [†]	Model Parameters					
					Age(Gyr)	$\tau^{\dagger\dagger}$	A_v	Z/Z_{\odot}	χ^2	z_f
12-6131	1.308	19.2	4.2	10.9	$0.8^{+0.6}_{-0.3}$	0.0	0.8	1.00	1.4	1.6
02-1255	1.340	18.3	4.7	11.2	$1.0^{+1.7}_{-0.3}$	0.0	0.8	1.75	1.9	1.8
02-1842	1.342	18.7	4.3	10.9	$0.9^{+0.7}_{-0.2}$	0.0	0.6	1.75	1.9	1.7
12-5836	1.348	18.9	3.6	10.7	$0.5^{+0.1}_{-0.1}$	0.0	0.6	1.30	3.6	1.5
15-7972	1.361	19.1	4.0	10.8	$2.0^{+2.5}_{-1.4}$	0.0	0.2	0.30	1.6	2.2
22-2587	1.395	19.3	4.1	10.7	$1.5^{+2.9}_{-0.8}$	0.0	0.0	1.00	1.6	2.5
22-0948	1.396	18.9	4.3	10.8	$4.0^{+0.4}_{-3.5}$	0.5	0.0	0.75	1.6	> 5
12-8025	1.397	18.9	4.2	11.1	$0.8^{+0.6}_{-0.1}$	0.0	0.0	1.75	2.2	1.8
22-0107	1.450	18.3	4.9	11.3	$3.2^{+0.7}_{-2.8}$	0.5	0.4	0.75	1.3	> 5
22-1983	1.488	19.1	4.6	11.1	$1.1^{+3.1}_{-0.5}$	0.0	0.0	1.30	1.3	2.1
22-0189	1.490	18.1	4.8	11.5	$3.0^{+0.7}_{-0.2}$	0.5	0.4	0.75	1.9	4.8
22-0674	1.493	18.8	4.4	11.1	$3.4^{+0.3}_{-1.7}$	0.5	0.0	0.75	1.6	> 5
12-5869	1.510	18.6	2.6	11.5	$1.2^{+0.6}_{-0.2}$	0.0	0.8	0.25	2.0	2.2
12-6072	1.576	19.8	4.3	10.8	$1.6^{+2.1}_{-1.3}$	0.2	0.2	0.75	2.0	2.7
12-5592	1.623	19.4	3.9	11.1	$1.1^{+0.3}_{-0.4}$	0.1	0.0	0.75	3.0	2.3
12-8895	1.646	18.5	4.7	11.5	$2.6^{+0.3}_{-0.3}$	0.5	0.4	0.75	2.2	4.7
15-4367	1.725	19.5	4.1	10.7	$2.1^{+0.4}_{-0.9}$	0.0	0.0	0.20	2.4	3.8
15-7543	1.801	19.0	4.6	11.0	$0.9^{+0.5}_{-0.2}$	0.0	0.0	1.75	1.9	2.4
15-5005	1.845	19.6	4.0	10.8	$0.5^{+0.7}_{-0.1}$	0.1	0.2	0.74	2.4	2.2
12-7672	2.147	19.1	4.4	11.1	$1.2^{+0.1}_{-0.4}$	0.1	0.0	0.74	2.0	3.4

[†] $\log_{10} M_*/M_{\odot}$ from Glazebrook et al. 2004 (Paper III)

^{††} e -folding time of star formation rate in Gyr.